Available online at www.sciencedirect.com
SCIENCE DIRECT®
Biochemical and Biophysical Research Communications 313 (2004) 559–567
BBRC
www.elsevier.com/locate/ybbrc

Binding of prion proteins to lipid membranes☆

Peter Critchley, Jurate Kazlauskaite, Robert Eason, and Teresa J.T. Pinheiro*

Department of Biological Sciences, University of Warwick, Gibbet Hill Road, Coventry CV4 7AL, UK

Received 10 November 2003

Abstract

A key molecular event in prion diseases is the conversion of the normal cellular form of the prion protein (PrP^C) to an aberrant form known as the scrapie isoform, PrP^{Sc}. Under normal physiological conditions PrP^C is attached to the outer leaflet of the plasma membrane via a GPI-anchor. It has been proposed that a direct interaction between PrP and lipid membranes could be involved in the conversion of PrP^C to its disease-associated corrupted conformation, PrP^{Sc}. Recombinant PrP can be refolded into an α-helical structure, designated α-PrP isoform, or into β-sheet-rich states, designated β-PrP isoform. The current study investigates the binding of recombinant PrP isoforms to model lipid membranes using surface plasmon resonance spectroscopy. The binding of α- and β-PrP to negatively charged lipid membranes of POPG, zwitterionic membranes of DPPC, and model raft membranes composed of DPPC, cholesterol, and sphingomyelin is compared at pH 7 and 5, to simulate the environment at the plasma membrane and within endosomes, respectively. It is found that PrP binds strongly to lipid membranes. The strength of the association of PrP with lipid membranes depends on the protein conformation and pH, and involves both hydrophobic and electrostatic lipid–protein interactions. Competition binding measurements established that the binding of α-PrP to lipid membranes follows a decreasing order of affinity to POPG > DPPC > rafts.

Keywords: Prion protein; Raft membranes; SPR

Transmissible spongiform encephalopathies (TSEs), also known as prion diseases, are associated with the conversion of the benign cellular form of the prion protein (PrP^C) into an infectious scrapie isoform (PrP^{Sc}) [1]. The transition between the cellular form and PrP^{Sc} occurs by an unidentified post-translational mechanism and appears to take place without any detectable covalent modifications to the protein molecule. A large body of experimental evidence indicates that the fundamental difference between the two forms of PrP resides in their conformation, which results in considerable differences in their physicochemical properties. PrP^C is rich in α-helical structure, monomeric, and susceptible to enzyme digestion, whereas PrP^{Sc} has a large content of β-sheet, forms highly insoluble aggregates, and is partially resistant to proteolytic digestion [2,3]. It is apparent that a major refolding event underlying the conversion of PrP^C to PrP^{Sc} plays a key role in the pathogenesis of prion diseases [4]. However, the molecular details of this conformational transition are not clearly understood.

The prion is a N-glycosylated protein, which occurs predominantly in neurons where it is anchored to the plasma membrane via a glycosyl phosphatidylinositol (GPI) anchor [5]. Several experimental observations [6–9] suggest that an interaction of PrP with the membrane surface may play a role in the conversion of PrP^C to PrP^{Sc}. In particular, the fact that PrP^C is released from the cell surface after digestion with phosphatidylinositol-specific phospholipase C (PIPLC) and PrP^{Sc} is not after similar treatment [7,8] strongly supports the idea that an altered membrane association of PrP may be an important factor in the mechanism of prion diseases.

☆ *Abbreviations:* CD, circular dichroism; chol, cholesterol; DPPC, dipalmitoylphosphatidylcholine (1,2-dipalmitoyl-*sn*-glycero-3-phosphocholine); EM, electron microscopy; lyso-PC, monoacyl-glycerophosphocholine; lyso-PS, monoacyl-glycerophosphoserine; MOG, monooleoylglycerol; PrP, prion protein; POPG, palmitoyloleoylphosphatidylglycerol (1-palmitoyl-2-oleoyl-*sn*-glycero-3-phospho-*rac*-(1-glycerol)); SHaPrP, Syrian hamster prion protein; SM, sphingomyelin; SPR, surface plasmon resonance.

* Corresponding author. Fax: +44-24-7652-3701.
E-mail address: T.Pinheiro@warwick.ac.uk (T.J.T. Pinheiro).

0006-291X/$ - see front matter © 2003 Elsevier Inc. All rights reserved.
doi:10.1016/j.bbrc.2003.12.004

Like other GPI-anchored proteins, PrP^{C} is segregated into cholesterol and sphingomyelin-rich domains or lipid rafts in the plasma membrane [10–12] from where its metabolic fate is determined. From the plasma membrane PrP^{C} can be recycled, degraded or possibly converted to PrP^{Sc}. The subcellular site for the formation of PrP^{Sc} is unknown; however, conversion occurs after PrP^{C} reaches the plasma membrane [13,14]. A recent study of PrP conversion in a cell-free system utilising purified raft membranes showed that conversion of raft-associated GPI-anchored PrP^{C} to PrP^{Sc} requires insertion of PrP^{Sc} into the lipid membrane [15]. Evidence from scrapie-infected cultured cells implicates the plasma membrane and endocytic organelles as relevant sites, but it is unclear which provides a more favourable environment for conversion and whether compartments along the secretory pathway might also be involved. Once PrP^{Sc} is formed, it appears to accumulate in late endosomes, lysosomes, and on the cell surface [12,16,17] or in extracellular spaces in the form of amorphous deposits, diffuse fibrils or dense amyloid plaques [18].

In addition to fully secreted GPI-anchored PrP, anchorless forms of PrP have been shown to be produced in the ER or released as soluble forms. Two transmembrane forms of PrP, either with the amino- or carboxy-terminus in the lumen, are associated with the ER membrane via a common transmembrane segment comprising residues 113–135 [19,20]. Release of soluble forms of PrP (lacking GPI anchor) from cells was first reported some years ago [21–24]. More recently, similar results have been obtained using splenocytes or cerebellar granule neurons from transgenic mice overexpressing PrP [25]. Also, it has been reported that 10–20% of PrP^{Sc} molecules extracted from infected hamsters are truncated at Gly228 and therefore lacking GPI anchor [26].

The majority of PrP^{Sc} generated in infected animals contains a GPI anchor and the relevance of anchorless forms of PrP is not clear. However, it is possible that anchorless forms of PrP may be physiologically relevant in the conversion process of PrP. A recent study has tested the effect of GPI anchor on prion conversion [27]. This work shows that either GPI-anchored (GPI^{+}) PrP or an anchor-deficient (GPI^{-}) form of PrP expressed in fibroblasts is stably associated with rafts, and the latter alternative mode of membrane association (independent of GPI) was not detectably altered by glycosylation and was not markedly reduced by deletion of the N-terminus. Furthermore, using a cell-free conversion assay, it was found that GPI^{+} PrP was not converted to PrP^{Sc} without the action of PIPLC or addition of the membrane-fusion agent polyethylene glycol (PEG), whereas GPI^{-} PrP was converted without PIPLC or PEG treatment. These findings support the view that additional direct lipid–polypeptide interactions may play a role in the conversion of PrP^{C} to PrP^{Sc}.

Recombinant PrP can be refolded as a predominantly α-helical conformation, designated α-PrP, or forms rich in β-sheet structure, designated β-PrP isoforms. Whereas α-PrP is monomeric and susceptible to enzyme digestion, β-PrP isoforms are oligomeric, partially resistant to proteolytic digestion, and form insoluble aggregates and fibrils [28]. Thus, recombinant β-sheet forms of PrP have properties of intermediate conformations of PrP that lead to PrP^{Sc}. In previous studies we have characterised the interaction of α- and β-isoforms of the truncated protein PrP(90–231) to model lipid membranes, both at pH 7 and 5, to model the pH environment of the plasma membrane and within endosomes, respectively [29,30]. These studies showed that α- and β-PrP have different binding affinities to lipid membranes and exhibit a different pH-dependent binding behaviour. The key findings, resulting from a combination of fluorescence, CD, FTIR, and EM studies, were that: (a) binding of α- and β-PrP to negatively charged lipid membranes results in increased β-sheet structure in PrP, which destabilises the lipid membrane and leads to amorphous aggregates of PrP; (b) binding of α-PrP to raft membranes increases α-helical structure, which does not destabilise the lipid membrane and does not lead to PrP aggregation; and (c) binding of β-PrP to rafts partially unfolds PrP, which does not destabilise the lipid membrane but leads to fibrillisation of PrP.

In the current study we investigate the binding of α-PrP to lipid membranes using surface plasmon resonance (SPR). Binding measurements were carried at pH 7 to represent the pH surrounding the plasma membrane, and at pH 5 to model the acidic environment of endocytic vesicles. The binding of PrP to membranes was studied with model lipid membranes composed of a single lipid or a mixture of lipids. Single lipid vesicles composed of negatively charged lipid, palmitoyloleoylphosphatidylglycerol (POPG), or zwitterionic lipid, dipalmitoylphosphatidylcholine (DPPC), were employed to identify the electrostatic and hydrophobic modes of interaction of PrP to lipid membranes. Mixed membranes composed of DPPC, cholesterol, and sphingomyelin (SM) were used to model the composition of rafts, where PrP accumulates in the plasma membrane.

Materials and methods

Materials. Cholesterol, POPG, and sphingomyelin were purchased from Avanti Polar Lipids (Alabaster, AL). DPPC and MOG were from Sigma–Aldrich (Dorset, UK).

Expression, purification, and refolding of PrP. Syrian hamster recombinant prion protein SHaPrP(90–231) was expressed using an alkaline phosphatase promoter in a protease-deficient strain of *Escherichia coli* (27C7) [31] and purified as described previously [29,30]. PrP was refolded into an α-helical conformation (α-PrP) or to a state with a higher content of β-sheet structure (β-PrP) [30]. The purity

of the final product was determined by SDS–polyacrylamide gel electrophoresis and electrospray ionisation mass spectrometry. Refolded PrP was dialysed against 5 mM Mes, pH 5.5, and stored in small aliquots. Protein samples were thawed prior to measurements, diluted into the appropriate buffer (10 mM Hepes, pH 5 or 7), and used on the same day. PrP concentration was determined spectrophotometrically using a molar extinction coefficient $\in_{280}$ of 24,420 M^{-1} cm^{-1} [32].

Preparation of lipid vesicles. Small unilamellar lipid vesicles were prepared by hydrating the required amount of dried lipid with the desired buffer; 10 mM Hepes at pH 7 or 5.0. Buffers were deoxygenated with nitrogen gas and the hydrated lipids were maintained under a nitrogen atmosphere. Phospholipids in chloroform solutions were dried under a rotary evaporator and the resulting lipid film was left under vacuum overnight to remove all traces of organic solvent. For the preparations of mixed lipid membranes, lipids were co-dissolved in chloroform or chloroform/methanol and a lipid film formed as described above. After lipid hydration the resulting multilamellar liposome suspension was sonicated in a bath sonicator until a clear suspension of small unilamellar vesicles was obtained (typically $6 \times 1/2$ h periods). Before deposition on the SPR chip, lipid suspensions were subjected to several cycles of vortexing and warming at 40 °C.

SPR measurements. SPR binding studies of PrP to various lipid membranes were performed at 25 °C on a Biacore 2000 instrument using the Biacore pioneer chip L1. The gold surface of the L1 chip is coated with a dextran layer containing lipophilic molecules for efficient capture of lipid vesicles onto the surface, resulting in an extended lipid bilayer over the dextran layer. The chip was equilibrated at 25 °C in 10 mM Hepes buffer with no sodium chloride, cleaned with 40 mM octyl glucoside (40 μL), and washed thoroughly with Hepes buffer. Lipid vesicles were deposited on the L1 chip by injecting 4×100 μL of their aqueous suspensions containing 0.5 mM lipid, washed with 2×50 mM NaOH to stabilise the deposited lipid layer and followed by a buffer injection to remove alkali. Fresh solutions of prion in Hepes buffer were injected at various concentrations (5–200 nM). To eliminate non-specific interactions, 50 μL of bovine serum albumin (BSA) solution (1 mg/mL) was flowed over the prepared chip before applying the prion solutions. For a given series of measurements varying prion concentration, the same lipid-coated surface was reused after alkali regeneration for as long as a consistent baseline was maintained. We found that using BSA to block non-specific adsorption sites on the dextran surface also helped us to maintain a consistent lipid surface that could be regenerated with two pulses of 50 mM NaOH. Typically, 100 μL injections were applied at a flow rate of 30 μL/min.

For the measurements of inhibition of binding of PrP to lipid membranes in the presence of NaCl, PrP was diluted from its stock solution to 200 nM in the required buffer containing increasing concentrations of NaCl (0–100 mM) and allowed to equilibrate for a few minutes before application over the lipid-coated chip. The deposition of lipid membranes on the L1 chip for the NaCl inhibition measurements was performed as above at the required pH, but washed with buffer containing the required NaCl concentration prior to the injection of the prion solution and during the desorption phase. The competition measurements with DPPC, POPG, and MOG were carried in a similar manner as described for NaCl inhibition, using the following ranges of competitor concentrations: DPPC (0–200 nM), POPG (0–175 nM), and MOG (0–50 nM) with a constant prion protein concentration of 200 nM.

A semi-quantitative comparative analysis of the association rates of PrP to lipid membranes was performed using a non-kinetic linear fitting model. In this analysis the rate of association is derived from the gradient of the association part of the sensorgram. Only the section of the sensorgrams up to one-third from the completion of injection of the association phase was selected for the determination of the gradient, where the *on* and *off* rates are close to a steady state and the surface is approaching saturation or has been saturated with prion.

Results

Binding of PrP to lipid membranes

Recombinant PrP(90–231) can be refolded from *E. coli* inclusion bodies either as an α-helical conformation (α-PrP) or a state with a higher content of β-sheet structure (β-PrP). Refolding under oxidising conditions yields the α-PrP isoform, which shows a characteristic far-UV CD spectrum with well-defined minima at 208 and 222 nm and a FTIR spectrum with a predominant amide I band ~1656 cm^{-1} [30]. In contrast, refolding of PrP(90–231) under reducing conditions produces a β-PrP isoform which shows a far-UV CD spectrum with a minimum ~218 nm and an intense amide I band ~1626 cm^{-1}, which are spectral signatures of β-sheet structure [30]. Peak fitting analysis of the amide I band revealed that α-PrP has 37% α-helix, 22% random coil, and 9.5% β-sheet, in good agreement with the NMR structure [33]. β-PrP has a lower content of α-helical structure (21%), a high content of β-sheet (35%), and only 4% random coil. The secondary structure content of β-PrP is overall analogous to the secondary structure of the proteinase K-resistant core of PrP extracted from tissues of diseased animals [2].

In surface plasmon resonance (SPR) a signal is produced when light is reflected from a thin layer of gold on the chip surface due to differences in refractive index arising from a deposited layer on the face of the gold opposite to that of the incident light. SPR causes a reduction in the intensity of reflected light at a specific angle of reflection and an SPR response is detected in resonance units (RU). Plotting the SPR response against time during the course of an interaction provides a quantitative measure of the progress of the interaction, and this plot is called a sensorgram. Typical sensorgrams for the interaction of α-PrP with lipid membranes deposited on a L1 sensor chip are shown in Fig. 1. The first phase of increasing response signal corresponds to the association of PrP to the deposited lipid membrane, followed by a phase of decreasing SPR signal corresponding to the dissociation of PrP. With all lipid membranes a strong association is observed followed by weak dissociation when buffer alone is injected. Regeneration of the chip surface is achieved with alkali washes.

Recombinant prion protein SHaPrP(90–231) has a net positive charge of +9 at pH 5 and +4 at pH 7. Positively charged residues are clustered on the protein surface, predominantly at the side of the protein molecule comprising the N-terminus, leaving the opposite side of the molecule with a more hydrophobic surface [29]. PrP must then be regarded as a multivalent analyte containing several clustered ionic sites as well as hydrophobic faces. This complex nature of PrP combined with the poor dissociation of α-PrP from lipid

membranes (Fig. 1) hampers our data analysis at a full kinetic level. Without an accurate estimation of the number of binding sites in PrP, calculation of molar rate constants for the association (k_a) and dissociation (k_d) of PrP to lipid membranes was difficult and, therefore, it was not possible to derive the equilibrium constants for association (K_A) and dissociation (K_D) of PrP. Instead, a semi-quantitative comparative analysis of the binding of PrP to lipid membranes is presented.

Based on a non-kinetic linear analysis the rate of association can be derived from the gradient of the association phase of the sensorgram. A summary of the association of α-PrP to single lipid membranes of POPG or DPPC, and raft membranes composed of DPPC, cholesterol, and sphingomyelin (DPPC/chol/SM, 50:30:20, molar ratio) at pH 7 and 5 is presented in Fig. 2. The binding rate of α-PrP to the three types of lipid membranes studied here is very similar at a given pH, but the level of PrP association is higher at pH 5 than at pH 7 (at pH 7 SPR response values are half of those observed at pH 5; Fig. 2).

Binding of the β-PrP isoform to lipid membranes of POPG, DPPC, and rafts shows a much stronger association than that observed with the α-PrP isoform (Fig. 3). The gradient of the association phase of β-PrP to membranes has values twice of those observed for the

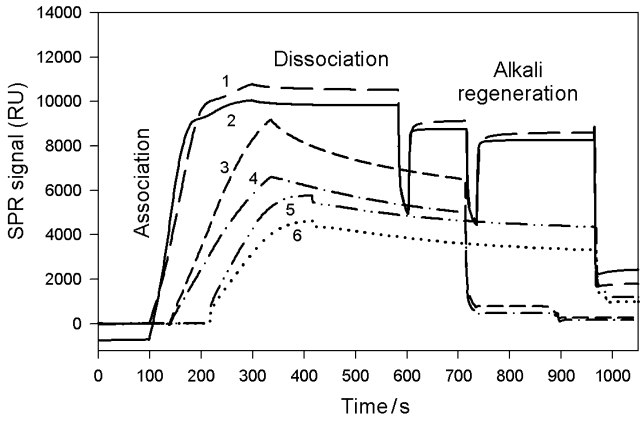

Fig. 1. Representative SPR sensorgrams for the binding of α-PrP to raft membranes (1, 3, 5) and DPPC (2, 4, 6). Top traces (1, 2) show a strong association phase and negligible dissociation at pH 5, followed by three pulses of alkali regeneration with 50 mM NaOH. Middle traces (3, 4) show binding and noticeable desorption at pH 7 followed by two pulses of alkali regeneration. Lower traces (5, 6) show the reduced association of PrP in the presence of 10 mM NaCl at pH 5. Lipid vesicles were immobilised on the surface of L1 sensor chip and PrP was presented from the mobile phase at a concentration of 200 nM.

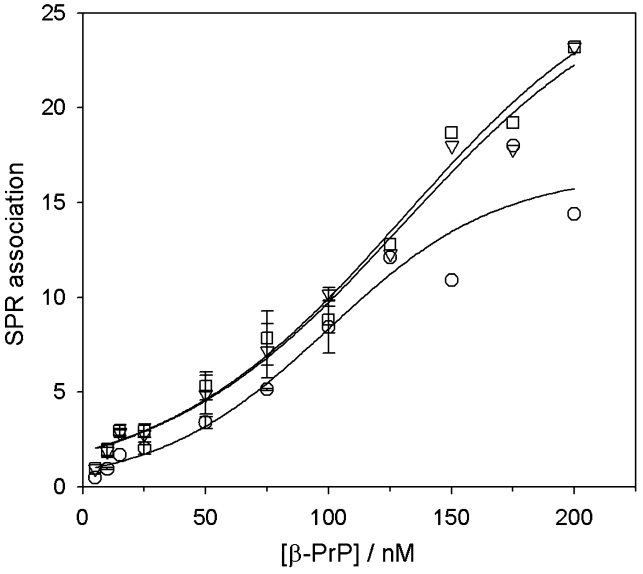

Fig. 3. The gradient of the association phase of SPR sensorgrams as a function of protein concentration for the binding of β-PrP to POPG (circles), rafts (squares), and DPPC membranes (triangles) at pH 7. Error bars represent the variation of 2–3 measurements.

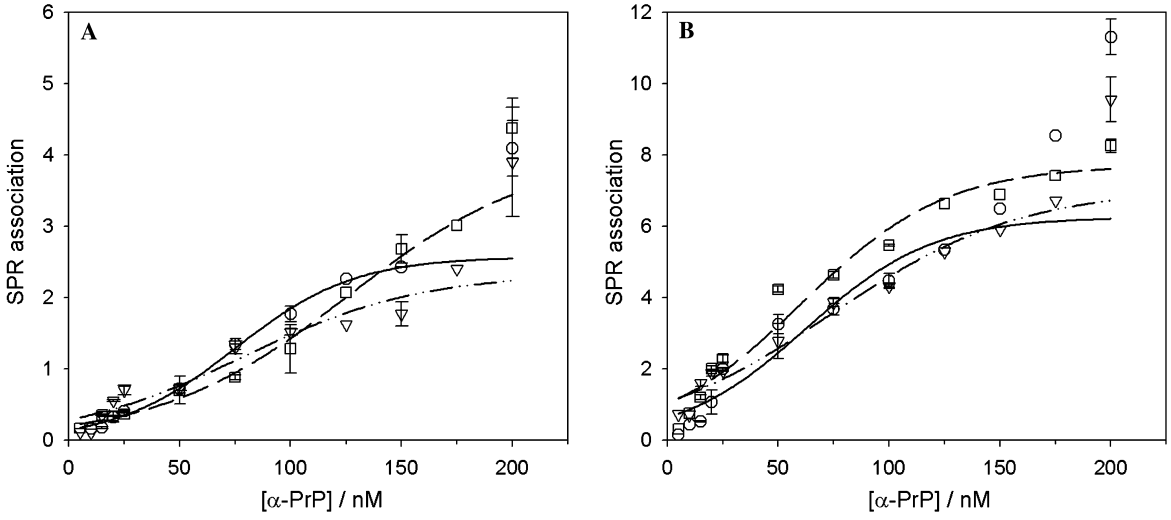

Fig. 2. The gradient of the association phase of SPR sensorgrams as a function of protein concentration for the binding of α-PrP to POPG (circles), rafts (squares), and DPPC membranes (triangles) at pH 7 (A) and pH 5 (B). Error bars represent the variation of 2–3 measurements.

association of α-PrP (Figs. 2 and 3). However, the binding of β-PrP to membranes was so strong that β-PrP could not be fully removed after alkali regeneration and membranes had to be stripped with 0.5% SDS after 9–10 protein injections and a new lipid surface prepared. Therefore, SPR measurements with β-PrP were limited.

Binding inhibition of NaCl

It has been suggested that binding of PrP to lipid membranes involves both electrostatic and hydrophobic interactions [29,30]. To further demonstrate the involvement of charge interactions in the binding of PrP to lipid membranes we have measured the SPR response signal for the interaction of α-PrP in the presence of increasing concentrations of NaCl. The effect of increasing concentrations of salt on the association of α-PrP to lipid membranes at pH 5 is shown in Fig. 4.

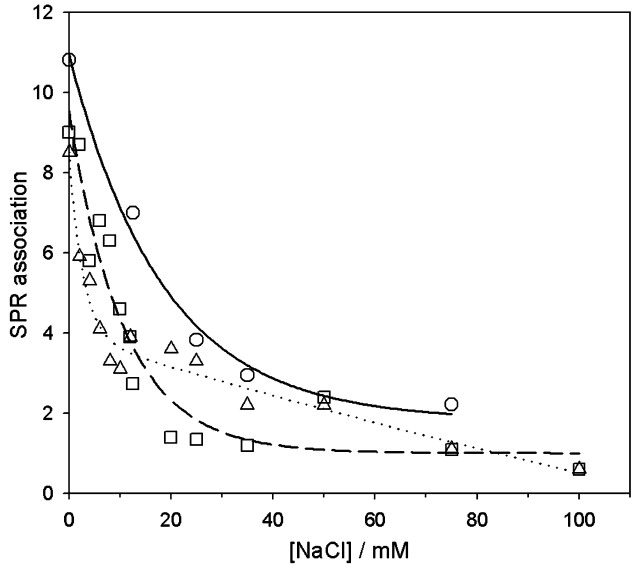

Fig. 4. The gradient of the association phase of SPR sensorgrams for the binding of α-PrP to POPG (circles), rafts (triangles), and DPPC membranes (squares) at pH 5 as a function of increasing concentrations of NaCl. Lipid vesicles were immobilised on the surface of L1 sensor chip and α-PrP (200 nM) was applied from the mobile phase in Hepes buffer containing increasing concentrations of NaCl.

Table 1
IC_{50} for the inhibition of binding of α-PrP to lipid membranes[a]

Inhibitor	Lipid vesicles		
	POPG	Rafts	DPPC
NaCl	100×10^{3}	50×10^{3}	25×10^{3}
MOG	5×10^{-2}	5×10^{-2}	5×10^{-2}
DPPC	50×10^{-2}	50×10^{-2}	5×10^{-2}
POPG	$<25 \times 10^{-3}$	$<25 \times 10^{-3}$	$<25 \times 10^{-3}$

[a] IC_{50} values are expressed in mol of inhibitor per mol of prion protein and were calculated from salt inhibition and competition measurements described in Results.

Membranes of POPG show a 50% reduction in the association of PrP at a concentration of NaCl ~20 mM. An equivalent reduction in the binding of α-PrP to DPPC and raft membranes occurs at lower salt concentrations ~10 and ~5 mM NaCl, respectively. The salt inhibition effects are expressed in Table 1 as inhibitory concentrations for 50% binding inhibition (IC_{50}) in moles of inhibitor per of mole of PrP.

Binding competition measurements

To establish the relative affinities of α-PrP to the different types of membranes and identify the relative strengths of hydrophobic and ionic components in the association of α-PrP with membranes, a series of competition measurements were performed. Low concentrations of free lipid ($\leqslant 200$ nM) pre-incubated with a fixed concentration of PrP (200 nM) were used to investigate their effects as competitive inhibitors to lower or prevent binding of α-PrP to a given membrane deposited on the chip. The competition of the neutral lipid, monooleoylglycerol (MOG), zwitterionic diacyl lipid, DPPC, and negatively charged diacyl lipid, POPG, was investigated for their relative inhibitory effects to the binding of α-PrP to POPG, DPPC, and raft membranes (Fig. 5). MOG has a similar inhibition effect on the binding of α-PrP to all three types of membranes, showing ~90% inhibition at a concentration of only 50 nM MOG (Fig. 5A). Near 80% inhibition of binding is achieved with 200 nM DPPC (Fig. 5B) and ~90% inhibition is observed with 200 nM POPG (Fig. 5C). Similar inhibition curves were observed for the three types of membranes for MOG (Fig. 5A) with an IC_{50} $\sim 5 \times 10^{-2}$ mol of MOG/mol of α-PrP (Table 1), indicating that a similar hydrophobic component is present in the three types of membranes and equally eliminated by the competitive interaction with MOG. Inhibition with DPPC resulted in similar curves for POPG and raft membranes (Fig. 5B) with an IC_{50} $\sim 50 \times 10^{-2}$ mol of DPPC/mol of α-PrP (Table 1), indicating that a similar zwitterionic component in the interaction of α-PrP with POPG and raft membranes is similarly eliminated by the competitive binding of monomeric DPPC to α-PrP. POPG is the most effective competitive inhibitor with an $IC_{50} < 25 \times 10^{-3}$ mol of POPG/mol of α-PrP (Table 1), indicating that the affinity of α-PrP to POPG is higher than that to DPPC and raft membranes.

Discussion

Previous studies have suggested that a direct interaction of PrP with the plasma membrane, other than via its GPI anchor, might play a role in the conversion of PrP^{C} to PrP^{Sc} [7,8,15,27]. From these studies it is

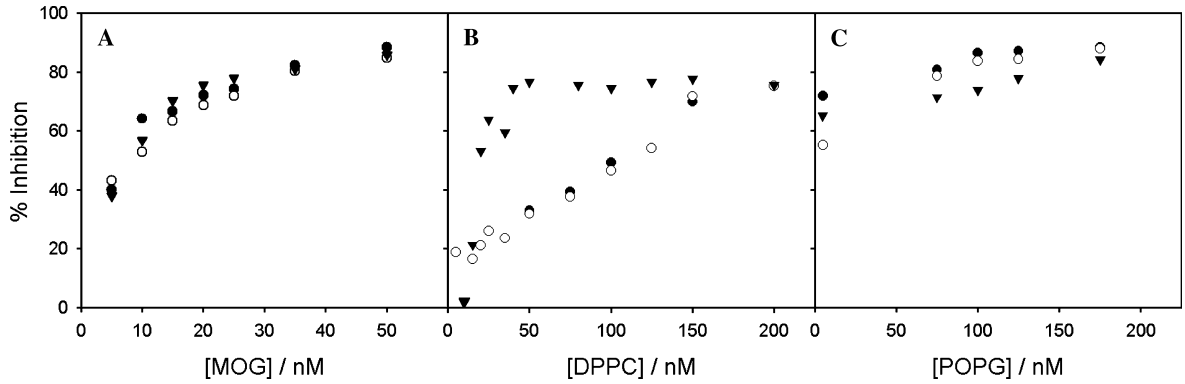

Fig. 5. Inhibition of MOG (A), DPPC (B), and POPG (C) to the binding of α-PrP to POPG (filled circles), rafts (open circles), and DPPC membranes (triangles). Lipid vesicles were immobilised on the surface of L1 sensor chip. Solutions of 200 nM PrP were pre-incubated in Hepes buffer containing increasing concentrations of inhibitor and presented to the immobilised lipid from the mobile phase. Before injection of PrP the deposited lipid membrane on the chip was washed with buffer containing the corresponding concentrations of inhibitor.

unknown whether the interaction of PrP with membranes would occur with the starting PrP^{C} conformation, which would become somehow altered by the association with lipid molecules or with an intermediate conformation of PrP primed for conversion, which results in PrP^{Sc} itself having an aberrant interaction with the plasma membrane. In order to understand how an interaction of PrP with lipid membranes might be involved in the conversion process of PrP, it is first necessary to identify the binding properties of PrP to lipid membranes. However, very few studies have been devoted to characterising the interaction of PrP with lipid membranes. Morillas et al. [34] showed that the interaction of recombinant human PrP requires a negatively charged lipid using mixed micelles of lyso-PC/lyso-PS. This interaction was found to be pH-dependent becoming particularly strong under acid conditions. Our previous studies have investigated the interaction of recombinant Syrian hamster PrP with lipid vesicles, both for the α-helical isoform, α-PrP [29] and the β-sheet enriched form, β-PrP [30].

Our current SPR study of the interaction of PrP with three types of lipid membranes, single lipid membranes of negatively charged lipid POPG or zwitterionic DPPC, and mixed lipid raft membranes composed of DPPC, cholesterol, and sphingomyelin shows that α-PrP binds very similarly to all three types of membranes (Fig. 2). This interaction is stronger at pH 5 than at pH 7, in good agreement with previous findings [29,30,34]. However, in contrast with previous binding results using protein Trp fluorescence, where no binding was observed for α-PrP with raft membranes at pH 5 [29], here we find that α-PrP binds strongly to raft membranes at pH 5. This disparity might be explained by the experimental differences in the two studies. First, the Trp binding measurements employed sonicated vesicles, with their characteristic high membrane curvature, whilst in the current SPR study membranes are deposited on the L1 chip dextran layer as an extended planar bilayer. Second, the range of lipid-to-protein ratio is at least 100- to 5000-fold higher in SPR measurements, assuming a 50% deposition of lipid on the chip surface than in the Trp binding study. The different morphology of the lipid bilayer (curved vs. planar) results in differences in the hydrophobic and electrostatic components available for the interaction with proteins. The curvature in vesicles exposes more the hydrophobic core of the bilayer than in a planar membrane. In the planar lipid bilayer composed of a single charged lipid, such as POPG, headgroup–headgroup charge repulsions will diminish the thigh lipid packing and therefore make the hydrophobic domain of the bilayer readily available for the interaction with hydrophobic sites in a protein. On the other hand, in a planar zwitterionic bilayer the lipid molecules can be more tightly packed than in a vesicle, resulting in a more dense electrostatic membrane surface and a less available hydrophobic core of the bilayer for hydrophobic interactions with the protein.

We observed a stronger binding of α-PrP at pH 5 than at pH 7 with all three types of membranes studied here. Due to protonation and deprotonation of His residues in PrP, the protein has a large difference in its overall surface charges between pH 7 and 5, having a net positive charge of +9 at pH 5 and +4 at pH 7. This charge difference combined with the observation that binding is stronger at pH 5 than at pH 7 (Fig. 2) reveals a strong electrostatic interaction in the binding of α-PrP to lipid membranes. This result corroborates that observed previously for the binding of α-PrP to POPG membranes [29]. The finding that α-PrP binds also more strongly at pH 5 to zwitterionic DPPC and raft membranes reveals that a strong ionic interaction between charged residues on the protein surface and charges in the phosphocholine lipid headgroup is involved. These results indicate that with all membranes analysed here binding of PrP appears to be driven first by long-range

ionic interactions likely followed by hydrophobic lipid–protein interactions.

Competition binding measurements with MOG revealed a similar hydrophobic component on the interaction of α-PrP with the three types of lipid membranes studied (Fig. 5A). Thus, differences in the affinity of α-PrP to these membranes must result from variations in electrostatic components. Binding measurements in the presence of NaCl established that ionic interactions are most strong for POPG membranes, with an IC_{50} of 100×10^3 mol of NaCl per mol of PrP, followed by DPPC membranes with an IC_{50} of 50×10^3 mol of NaCl per mol of PrP (Table 1). In previous salt inhibition measurements of the binding of α-PrP to zwitterionic membranes, using vesicles and monitored by Trp fluorescence, little or no effect on the binding of α-PrP was observed [29]. This difference corroborates our interpretation that in planar zwitterionic membranes lipid molecules pack more tightly producing a denser ionic surface and therefore occluding the hydrophobic core of the lipid bilayer. Thus, in our current SPR study electrostatic interactions between PrP and DPPC or raft membranes appear stronger, as revealed by the salt inhibition effects. An extended planar bilayer might represent better the plasma membrane, whereas highly curved bilayers in small vesicles should serve as better models of endocytic vesicles.

Compared to DPPC membranes, a reduction in salt inhibition for the binding of α-PrP to rafts was observed (IC_{50} of 25×10^3 mol of NaCl per mole of PrP; Table 1), revealing a weaker electrostatic component on the interaction of α-PrP with rafts relative to the interaction with DPPC. Charge contributions in raft membranes arise from the phosphocholine moiety in DPPC and SM, but these are diluted by the presence of cholesterol, thus resulting in a lower membrane surface charge density compared to single lipid membranes of DPPC.

It is noteworthy that salt inhibition results show a biphasic decay, particularly noticeable with raft membranes (Fig. 4). PrP has a complex electrostatic surface potential with several clusters of charges interspaced with more hydrophobic patches [29]. Therefore, it is plausible that binding of PrP to a membrane results in a heterogeneous population of bound states, with protein molecules in different orientations relative to the membrane surface. In addition, it is anticipated that screening of charges with salt might facilitate hydrophobic lipid–protein interactions. Thus, the observed biphasic decay of the salt inhibition results might be associated with distinct binding modes of PrP with a lipid membrane, either involving different ionic interactions through diverse sites on the protein surface or hydrophobic lipid–protein interactions.

Experimental evidence from studies involving animal extracted PrP^{Sc} [7,8] and cell-free PrP conversion systems [15,27] suggests that PrP^{Sc} has an aberrant association with lipid membranes involving direct lipid–polypeptide interactions in addition to GPI anchor. The use of recombinant β-PrP isoform, which has some of the properties of PrP^{Sc} or of intermediate conformations of PrP that lead to the formation of PrP^{Sc}, serves to model the interaction of PrP^{Sc} with membranes.

The high SPR association response observed for the interaction of β-PrP with lipid membranes (Fig. 3) shows that β-PrP associates more strongly with membranes than the α-PrP isoform. It is pertinent to point out that plots of the gradient of the SPR association phase for β-PrP do not achieve saturation (Fig. 3). The observed increasing trend in the binding curves for β-PrP, combined with the high propensity of β-PrP to oligomerise and form larger aggregates and fibrils, suggests that binding of β-PrP carries on involving protein–protein interactions. This interpretation is corroborated by EM results where aggregation and fibrillisation of β-PrP was shown to occur in these membranes [30]. Plots of the gradient of the SPR association phase for α-PrP have a more defined binding saturation level (Fig. 2), but at higher protein concentrations (~200 nM) a deviation starts to appear, which may also be associated with the initiation of protein oligomerisation on the membrane surface. Aggregation of α-PrP with lipid membranes was also observed in EM measurements and was particularly strong with POPG membranes [30].

The binding of β-PrP was very strong at pH 5 and under these conditions β-PrP could not be dissociated from the membrane. A strong binding of β-PrP to lipid membranes is consistent with previous Trp binding results [30], where a pronounced binding enhancement of β-PrP to POPG and rafts was observed at pH 5 compared to pH 7. The overall effect of stronger association of both α- and β-PrP to lipid membranes at pH 5 suggests that endosomes and lysosomes, where the pH is more acidic than at the plasma membrane reaching values ~pH 5, can provide an environment conducive to strong association of PrP with the membrane surface. Depending on the starting conformation of PrP, this interaction can be irreversible and could result in drastic consequences. On a membrane-associated state, a PrP molecule destined for degradation can become more protected to proteolytic digestion and start to accumulate in the cell. Alternatively, because PrP is constitutively recycled between the endocytic compartment and the plasma membrane [35], a corrupted conformation generated in endosomes can appear at the plasma membrane where it could serve as a catalyst for the conversion of PrP^{C}.

In conclusion, it is apparent that long-range ionic lipid–protein interactions play a crucial role in the association of PrP with lipid membranes and are likely

to constitute the driving force for the initial binding. However, once on the membrane surface short-range hydrophobic lipid–protein interactions take place. These lipid–protein interactions can alter the protein conformation, which may result in a higher propensity for the association of PrP with other PrP molecules on the membrane surface. Thus, the two-dimensional confinement of PrP molecules on a membrane surface, coupled to acidic conditions such as in endosomes, may provide a favourable environment for the conversion of PrP.

Acknowledgments

This work has been supported by the Medical Research Council (G990445), the Biotechnology and Biological Sciences Research Council (88/BS516471), and the Royal Society.

References

[1] S.B. Prusiner, Prions, Proc. Natl. Acad. Sci. USA 95 (1998) 13363–13383.
[2] B.W. Caughey, A. Dong, K.S. Bhat, D. Ernst, S.F. Hayes, W.S. Caughey, Secondary structure analysis of the scrapie-associated protein PrP 27–30 in water by infrared spectroscopy, Biochemistry 30 (1991) 7672–7680.
[3] K.M. Pan, M.A. Baldwin, J. Nguyen, M. Gasset, A. Servban, D. Groth, I. Mehlhorn, Z. Huang, R.J. Fletterick, F.E. Cohen, S.B. Prusiner, Conversion of α-helices into β-sheets features in the formation of the scrapie prion proteins, Proc. Natl. Acad. Sci. USA 90 (1993) 10962–10966.
[4] B. Caughey, G.J. Raymond, M.A. Callahan, C. Wong, G.S. Baron, L.W. Xiong, Interactions and conversions of prion protein isoforms, Adv. Protein Chem. 57 (2001) 139–169.
[5] P.M. Rudd, M.R. Wormald, D.R. Wing, S.B. Prusiner, R.A. Dwek, Prion glycoprotein: structure, dynamics and roles for the sugars, Biochemistry 40 (2001) 3759–3766.
[6] R. Gabizon, M.P. McKinley, S.B. Prusiner, Purified prion proteins and scrapie infectivity copartition into liposomes, Proc. Natl. Acad. Sci. USA 84 (1987) 4017–4021.
[7] N. Stahl, D.R. Borchelt, S.B. Prusiner, Differential release of cellular and scrapie prion protein from cellular membranes by phosphatidylinositol-specific phospholipase C, Biochemistry 29 (1990) 5405–5412.
[8] J. Safar, M. Ceroni, D.C. Gajdusek, C.J. Gibbs, Differences in the membrane interaction of scrapie amyloid precursor proteins in normal and scrapie- or Creutzfeldt-Jakob disease-infected brains, J. Inf. Dis. 163 (1991) 488–494.
[9] S. Lehmann, D.A. Harris, A mutant prion protein displays an aberrant membrane association when expressed in cultured cells, J. Biol. Chem. 270 (1995) 24589–24597.
[10] N. Stahl, D.R. Borchelt, K. Hsiao, S.B. Prusiner, Scrapie prion protein contains a phosphatidylinositol glycolipid, Cell 51 (1987) 229–240.
[11] M. Vey, S. Pilkuhn, H. Wille, R. Nixon, S.J. DeArmond, E.J. Smart, R.G.W. Anderson, A. Taraboulos, S.B. Prusiner, Subcellular colocalisation of the cellular and scrapie prion proteins in caveolae-like membranous domains, Proc. Natl. Acad. Sci. USA 93 (1996) 14945–14949.
[12] N. Naslavsky, R. Stein, A. Yanai, G. Friedlander, A. Taraboulos, Characterisation of detergent-insoluble complexes containing cellular prion protein and its scrapie isoform, J. Biol. Chem. 272 (1997) 6324–6331.
[13] B. Caughey, G.J. Raymond, The scrapie-associated form of PrP is made from a cell surface precursor that is both protease- and phospholipase-sensitive, J. Biol. Chem. 266 (1991) 18217–18224.
[14] A. Taraboulos, M. Scott, A. Semenov, D. Avraham, L. Laszlo, S.B. Prusiner, Cholesterol depletion and modification of COOH-terminal targeting sequence of the prion inhibit formation of scrapie isoform, J. Cell Biol. 129 (1995) 121–132.
[15] G.S. Baron, K. Wehrly, D.W. Dorward, B. Chesebro, B. Caughey, Conversion of raft-associated prion protein to protease-resistant state requires insertion of PrP-res (PrP^{Sc}) into contiguous membranes, EMBO J. 21 (2002) 1031–1040.
[16] B. Caughey, Cellular metabolism of normal and scrapie-associated forms of PrP, Sem. Virol. 2 (1991) 189–196.
[17] S.L. Shyng, M.T. Huber, D.A. Harris, A prion protein cycles between the cell surface and an endocytic compartment in cultured neuroblastoma cells, J. Biol. Chem. 268 (1993) 15922–15928.
[18] S.J. DeArmond, S.B. Prusiner, Etiology and pathogenesis of prion diseases, Am. J. Pathol. 146 (1995) 785–811.
[19] B. Hay, R.A. Barry, I. Lieberburg, S.B. Prusiner, V.R. Lingappa, Biogenesis and transmembrane orientation of the cellular isoform of the scrapie prion protein, Mol. Cell. Biol. 7 (1987) 914–920.
[20] C.D. Lopez, C.S. Yost, S.B. Prusiner, R.M. Myers, V.R. Lingappa, Unusual topogenic sequence directs prion protein biogenesis, Science 248 (1990) 226–229.
[21] B. Caughey, R.E. Race, M. Vogel, M.J. Buchmeier, B. Chesebro, In vitro expression in eukaryotic cells of a prion protein gene cloned from scrapie-infected mouse brain, Proc. Natl. Acad. Sci. USA 85 (1988) 4657–4661.
[22] B. Caughey, R.E. Race, D. Ernst, M.J. Buchmeier, B. Chesebro, Prion protein biosynthesis in scrapie-infected and uninfected neuroblastoma cells, J. Virol. 63 (1989) 175–181.
[23] D.R. Borchelt, M. Scott, A. Taraboulos, N. Stahl, S.B. Prusiner, Scrapie and cellular prion proteins differ in their kinetics of synthesis and topology in cultured cells, J. Cell Biol. 110 (1990) 743–752.
[24] D.R. Borchelt, M. Rogers, N. Stahl, G. Telling, S.B. Prusiner, Release of the cellular prion protein from cultured cells after loss of its glycoinositol phospholipid anchor, Glycobiology 3 (1993) 319–329.
[25] P. Parizek, C. Roeckl, J. Weber, E. Flechsig, A. Aguzzi, A.J. Raeber, Similar turnover and shedding of the cellular prion protein in primary lymphoid and neuronal cells, J. Biol. Chem. 276 (2001) 44627–44632.
[26] N. Stahl, M.A. Baldwin, A.L. Burlingame, S.B. Prusiner, Identification of glycoinositol phospholipid linked and truncated forms of the scrapie prion protein, Biochemistry 29 (1990) 8879–8884.
[27] G.S. Baron, B. Caughey, Effect of GPI anchor-dependent and -independent PrP association with model raft membranes on conversion to the protease-resistant isoform, J. Biol. Chem. 278 (2003) 14883–14892.
[28] I.V. Baskakov, G. Legname, M.A. Baldwin, S.B. Prusiner, F.E. Cohen, Pathway complexity of prion assembly into amyloid, J. Biol. Chem. 277 (2002) 21140–21148.
[29] N. Sanghera, T.J.T. Pinheiro, Binding of prion protein to lipid membranes and implications for prion conversion, J. Mol. Biol. 315 (2002) 1241–1256.
[30] J. Kazlauskaite, N. Sanghera, I. Sylvester, C. Vénien-Bryan, T.J.T. Pinheiro, Structural changes of the prion protein in lipid membranes leading to aggregation and fibrillization, Biochemistry 42 (2003) 3295–3304.
[31] I. Mehlhorn, D. Groth, J. Stockel, B. Moffat, D. Reilly, D. Yansura, W.C. Willett, M.A. Baldwin, R. Fletterick, F.E. Cohen,

R. Vandlen, D. Henner, S.B. Prusiner, High-level expression and characterisation of a purified 142-residue polypeptide of the prion protein, Biochemistry 35 (1996) 5528–5537.

[32] S.C. Gill, P.H. Hippel, Calculation of protein extinction coefficients from amino acid sequence data, Anal. Biochem. 182 (1989) 319–326.

[33] T.L. James, H. Liu, N.B. Ulyanov, S. Farr-Jones, H. Zhang, D.G. Donne, K. Kaneko, D. Groth, I. Mehlhorn, S.B. Prusiner, F.E. Cohen, Solution structure of a 142-residue recombinant prion protein corresponding to the infectious fragment of the scrapie isoform, Proc. Natl. Acad. Sci. USA 94 (1997) 10086–10091.

[34] M. Morillas, W. Swietnicki, P. Gambetti, W.K. Surewicz, Membrane environment alters the conformational structure of the recombinant human prion protein, J. Biol. Chem. 274 (1999) 36859–36865.

[35] C. Sunyach, A. Jen, J. Deng, K.T. Fitzgerald, Y. Frobert, J. Grassi, M.W. McCaffrey, R. Morris, The mechanism of internalization of glycosylphosphatidylinositol-anchored prion protein, EMBO J. 22 (2003) 3591–3601.